Published online 7 June 2018

Nucleic Acids Research, 2018, Vol. 46, No. 17 ***e101***
doi: 10.1093/nar/gky505

qEva-CRISPR: a method for quantitative evaluation of CRISPR/Cas-mediated genome editing in target and off-target sites

Magdalena Dabrowska[1,†], Karol Czubak[2,†], Wojciech Juzwa[3], Wlodzimierz J. Krzyzosiak[4], Marta Olejniczak[1,*] and Piotr Kozlowski[2,*]

[1]Department of Genome Engineering, Institute of Bioorganic Chemistry, Polish Academy of Sciences, Noskowskiego 12/14, 61-704 Poznan, Poland, [2]Department of Molecular Genetics, Institute of Bioorganic Chemistry, Polish Academy of Sciences, Noskowskiego 12/14, 61-704 Poznan, Poland, [3]Department of Biotechnology and Food Microbiology, Poznan University of Life Sciences, Wojska Polskiego 48, 60-627 Poznan, Poland and [4]Department of Molecular Biomedicine, Institute of Bioorganic Chemistry, Polish Academy of Sciences, Noskowskiego 12/14, 61-704 Poznan, Poland

Received April 04, 2018; Editorial Decision May 17, 2018; Accepted May 23, 2018

ABSTRACT

Genome editing technology based on engineered nucleases has been increasingly applied for targeted modification of genes in a variety of cell types and organisms. However, the methods currently used for evaluating the editing efficiency still suffer from many limitations, including preferential detection of some mutation types, sensitivity to polymorphisms that hamper mismatch detection, lack of multiplex capability, or sensitivity to assay conditions. Here, we describe qEva-CRISPR, a new quantitative method that overcomes these limitations and allows simultaneous (multiplex) analysis of CRISPR/Cas9-induced modifications in a target and the corresponding off-targets or in several different targets. We demonstrate all of the advantages of the qEva-CRISPR method using a number of sgRNAs targeting the *TP53*, *VEGFA*, *CCR5*, *EMX1* and *HTT* genes in different cell lines and under different experimental conditions. Unlike other methods, qEva-CRISPR detects all types of mutations, including point mutations and large deletions, and its sensitivity does not depend on the mutation type. Moreover, this approach allows for successful analysis of targets located in 'difficult' genomic regions. In conclusion, qEva-CRISPR may become a method of choice for unbiased sgRNA screening to evaluate experimental conditions that affect genome editing or to distinguish homology-directed repair from non-homologous end joining.

INTRODUCTION

Genome-editing technology is widely used to inactivate or modify specific genes in functional studies or in therapeutic approaches. The Clustered Regularly Interspaced Short Palindromic Repeats (CRISPR)/Cas9 system (1–4) recently became a major genome editing tool that has replaced previously developed zinc finger nucleases (ZFNs) and transcription activator-like effector nucleases (TALENs) (5,6). In the CRISPR/Cas9 system, single guide RNA (sgRNA) is used to guide the Cas9 nuclease to target DNA containing the protospacer adjacent motif (PAM), which is 5′-NGG-3′ for *Streptococcus pyogenes* Cas9. Double-strand breaks (DSBs) generated by Cas9 at ∼3 bp upstream from PAM are mainly repaired by error-prone non-homologous end joining (NHEJ), which results in a variety of scar mutations, most of which are insertion/deletion (INDEL) frameshift mutations leading to premature translation termination and transcript degradation by nonsense-mediated decay (NMD). Alternatively, the homology-directed repair (HDR) mechanism can repair the break precisely using a DNA repair template. The mechanism of CRISPR/Cas9-mediated genome editing has been recently described in detail in several excellent review articles, e.g. (7). There are four possible results of target gene editing in a single diploid cell: no mutation, heterozygous mutation (only one allele is mutated), homozygous mutation (the same mutation in both alleles), and biallelic mutation (different mutations on both alleles). Despite great progress in sgRNA design algorithms (8–10), the efficiency of a specific DSB induction within the target sequence is still difficult to predict. Additionally, unspecific targeting of other genomic regions (off-targets) is difficult to avoid and therefore remains one of the most im-

*To whom correspondence should be addressed. Tel: +48 61 8528503; Fax: +48 61 8520532; Email: kozlowp@ibch.poznan.pl
Correspondence may also be addressed to Marta Olejniczak. Tel: +48 61 8528503; Fax: +48 61 8520532; Email: marta.olejniczak@ibch.poznan.pl
†The authors wish it to be known that, in their opinion, the first two authors should be regarded as Joint First Authors.

portant challenges of genome editing approaches, especially in the context of their clinical applications [reviewed in (11)].

Several methods have been developed to evaluate the activity of sgRNAs and frequency of INDEL mutations; however, all of them have their specific limitations (12). Most methods, including mismatch cleavage assays, high-resolution melting analysis (HRMA), and heteroduplex mobility, are based on cleavage or modified migration of the heteroduplexes formed by mutated and wild-type DNA strands (6,13–15). These methods are widely used for preliminary screening of sgRNA activity due to their simplicity, low cost, and requirements for basic laboratory equipment. The most popular of these techniques utilize T7 endonuclease 1 (T7E1) or Surveyor nuclease (Transgenomic, Inc., USA) to cleave mismatches formed between modified and unmodified DNA strands (12,16). Despite these advantages, mismatch cleavage assays can overlook both single-nucleotide changes as well as larger deletions. They also cannot detect homozygous mutations and are not suitable for analyses of polymorphic loci (17). Other INDEL detection methods include restriction fragment length polymorphism (RFLP) (5,18), loss of a primer binding site (19), analysis of a PCR product length polymorphism (20), and decomposition of Sanger sequencing reads by TIDE (21,22) and CRISPR-GA (23). Alternative methods have also been proposed (24,25). Unlike heteroduplex-utilizing assays, these methods allow for detection of homozygous mutant clones. Most of the abovementioned methods take advantage of the principles of mutation detection methods that were developed and commonly used in the 1990s and are affected by their limitations, of which the most important are as follows: limited sensitivity (usually ∼80%), the confounding effects of common SNPs that frequently occur in the vicinity of the site of interest, and an inability to detect larger (>200) deletions/duplications. Most importantly, many of these methods were not designed to be quantitative and have limited or no multiplexing capabilities.

Functional screening of candidate sgRNAs rarely includes a more challenging analysis of off-targets. Although bioinformatics tools are helpful to predict potential sgRNA off-targets in the genome of interest [e.g. (12,26)], the number of off-targets may depend on many factors, including the thermodynamic properties of sgRNA and actual local concentrations of sgRNA and Cas9 as well as the local ion concentrations and presence of various specific and unspecific competing or sequestrating elements. The latter factor further depends on experimental conditions, such as the cell type or sgRNA/Cas9 delivery strategy [reviewed in (11)].

Here, we describe a new method for **q**uantitative **Eva**luation of **CRISPR**/Cas9-mediated editing (qEva-CRISPR) that allows for parallel analysis of target and selected off-target sites. qEva-CRISPR is a ligation-based dosage-sensitive method. It takes advantage of the previously developed and well-validated strategy of the multiplex ligation-based probe amplification (MLPA) assay design (27,28). The strategy exclusively utilizes short oligonucleotide probes that can be easily generated via standard chemical synthesis for any target of interest. The general concept of the MLPA method, which is mostly used for detection of large deletions in disease-related genes, has been described and reviewed previously (29,30).

Using the developed qEva-CRISPR assays, we quantitatively measured the efficiency of several sgRNAs in target and off-target sites in different human cell lines and under different conditions in CRISPR/Cas9 experiments. Among the analyzed targets were those located within low-complexity sequences flanking the CAG microsatellite tract in the *huntingtin* (*HTT*) gene, for which other assays could not be designed or did not work reliably. We demonstrate the ability of qEva-CRISPR to distinguish sequences generated by NHEJ and HDR.

MATERIALS AND METHODS

Plasmids

The sgRNA sequences E4.1 and E4.2, which are specific for target sequences within the *TP53* gene, and sgRNAs specific for the *VEGFA* (VEGFA), *EMX1* (EMX1), and *CCR5* (CCR5.1, CCR5.6, and CCR5.7) genes have been described previously (31–33). To generate the Cas9_E4.1, Cas9_E4.2, Cas9_VEGFA, Cas9_EMX1, Cas9_CCR5.1, Cas9_CCR5.6 and Cas9_CCR5.7 plasmids, sense and antisense DNA strands of sgRNAs were synthesized (IBB, Warsaw, Poland), annealed to each other, and ligated into the FastDigest BsmBI (Thermo Fisher Scientific, Waltham, MA, USA) digested pSpCas9(BB)-2A-GFP (PX458) (Addgene, Cambridge, MA, USA) plasmid. Chemically competent *Escherichia coli* GT116 cells (InvivoGen, San Diego, CA, USA) were transformed with the ligated plasmids, plated onto ampicillin selection plates (100 μg/ml ampicillin) and incubated overnight at 37°C. The plasmids were isolated using the Gene JET Plasmid Miniprep kit (Thermo Fisher Scientific) and analyzed by Sanger sequencing with the U6-Fwd primer. The same strategy was used to generate plasmids encoding Cas9 and three sgRNAs specific for the *HTT* gene (34): Cas9_HTT.sg1, Cas9_HTT.sg3 and Cas9_HTT.sg4. Two *HTT* sgRNAs were also used with the nickase version of Cas9 (Cas9n; D10A mutant; pSpCas9n(BB)-2A-GFP (PX461)): Cas9n_HTT.sg1 and Cas9n_HTT.sg4. The oligonucleotide sequences are presented in Supplementary Table S1.

Cell culture and transfection

Human colon cancer cells (HCT116), human embryonic kidney cells (HEK293T), human myeloid leukemia cells (K562) and HeLa cells were grown in Dulbecco's modified Eagle's medium (Lonza; Basel, Switzerland) supplemented with 10% fetal bovine serum (Sigma-Aldrich, Saint Louis, MS, USA), antibiotics (Sigma-Aldrich) and L-glutamine (Sigma-Aldrich). HCT116 and HeLa transfections were performed using Lipofectamine LTX (Life Technologies, Carlsbad, CA, USA) according to the manufacturer's instructions. Plasmids were transfected with a concentration of 0.25 μg to 2 μg/12-well plate. The transfection efficiency (GFP positive cells) was determined by flow cytometry (BD Accuri™ C6, BD Biosciences, Franklin Lakes, NJ, USA). HEK293T were transfected using the calcium phosphate method with 10 μg of plasmid DNA or 5 μg of each plasmid from a Cas9n_HTT.sg1 and Cas9n_HTT.sg4 pair for 3×10^5 cells/plate. HCT116 and K562 cells were electroporated with the Neon™ Transfection System (Invitrogen,

Carlsbad, CA, USA). Briefly, 0.5–1 × 10^5 cells were harvested, resuspended in Buffer R and electroporated with 1 μg of plasmid DNA in 10 μl tips using the following parameters: 1130 V, 30 ms, 2 pulses or 1450 V, 10 ms, 3 pulses for HCT116 and K562 cells, respectively. In multiplex analysis, the concentration of each plasmid DNA was either 200 ng (0.6 μg in total) or 330 ng (1 μg in total). In HDR experiments, the HEK293T cells were electroporated with 125 ng of plasmid DNA (62.5 ng of each Cas9n_HTT.sg1 and Cas9n_HTT.sg4 plasmids) and 0.5 μl of 10 μM oligodeoxynucleotide (ssODN) as a donor template (IDT, Skokie, IL, USA) (Supplementary Table S1) using the following parameters: 1150 V, 20 ms, 2 pulses. The cells were cultured for 48 hours, after which genomic DNA was isolated with the Cells and Tissue DNA Isolation Kit (Norgen, Biotek Corp., Schmon Pkwy, ON, Canada) according to the manufacturer's instructions.

In vitro T7 transcription of sgRNA and RNP complex delivery

R_1s and R_1a oligonucleotides corresponding to HTT_sg.1 (IBB, Warsaw) (Supplementary Table S1) were annealed and ligated into the FastDigest *Bpi*I (Thermo Fisher Scientific) digested p31 vector, which contains a T7 RNA polymerase promoter and Cas9 gRNA scaffold sequence. Chemically competent *E. coli* GT116 cells (InvivoGen) were transformed with the ligated plasmids, plated onto ampicillin selection plates (100 μg/ml ampicillin) and incubated overnight at 37°C. The plasmids were isolated using the Gene JET Plasmid Miniprep kit (Thermo Fisher Scientific) and analyzed by Sanger sequencing with the WSF6 primer. The sgRNA expression vectors were digested with FastDigest *Dra*I (Thermo Fisher Scientific), and the sgRNA was synthesized using an AmpliScribe T7-Flash Transcription Kit (Epicentre, Madison, WI, USA). The synthesized sgRNA was purified by phenol–chloroform–isoamyl alcohol (PanReac AppliChem, Barcelona, Spain) extraction and its integrity was checked by electrophoresis on a 10% PAA/urea/1× TBE gel.

The RNP complex was produced by mixing recombinant NLS-SpCas9-NLS nuclease (VBCF Protein Technologies facility http://www.vbcf.ac.at) and *in vitro* transcribed sgRNA. Cas9 RNPs were prepared immediately before electroporation by incubating 2.5, 5 and 10 μg of Cas9 protein with 6, 12 and 24 μg of sgRNA transcript in an appropriate buffer containing 200 mM HEPES (pH 7.5), 1.5 M KCl, 5 mM DTT and 1 mM EDTA at 37°C for 10 min. HEK293T cells were electroporated with a Neon transfection system (Invitrogen) according to the manufacturer's instruction.

Fluorescence-activated cell sorting

Cells were sorted using the BD FACSAria™ III (BD Biosciences) flow cytometer (cell sorter) 48 h post-electroporation. The configuration of the flow cytometer was as follows: a 100-μm nozzle and 20 psi (0.138 MPa) of sheath fluid pressure. Cells were characterized by two non-fluorescent parameters, forward scatter (FSC) and side scatter (SSC), and one fluorescent parameter, which was green fluorescence from GFP collected using the 530/30 band-pass filter (FITC detector). Data were acquired in a four-decade logarithmic scale as area signals (FSC-A, SSC-A, and FITC-A) and analyzed with FACS DIVA software (BD Biosciences). GFP-positive cells were divided into three fractions based on the fluorescence intensity. Each fraction contained ∼1–2 × 10^4 cells that were seeded onto a 6-well plate, maintained until confluence and collected for genomic DNA extraction.

Single-cell clones

To obtain single-cell clones, the HCT116 cells were transfected with the Cas9_E4.1 or Cas9_E4.2 plasmids, sorted by FACS and plated onto 150-mm cell plates to form single-cell clones. Individual colonies were picked with the use of cloning rings and transferred into 48-well plates according to the manufacturer's instructions (Promega, Madison, WI, USA). DNA was isolated from cells using 0.5 × Direct-Lyse buffer as described by Ramlee et al (30). PCR was performed using the MK024 and MK025 primers, and single-cell clones were genotyped by Sanger sequencing with the MK024 primer (Supplementary Table S1).

T7E1 mutation detection assay

For the T7E1 mismatch assay, genomic DNA was amplified using Phusion High-Fidelity PCR Master Mix (Thermo Fisher Scientific) with primers (MK024 and MK025) as described in the paper by Ramlee et al (30). The PCR amplification conditions were as follows: initial denaturation for 3 min at 95°C; 30 cycles of 95°C for 30 s, 63°C for 30 s, and 72°C for 30 s; and a final elongation at 72°C for 5 min. PCR products were purified using the GeneJET PCR Purification Kit (Thermo Fisher Scientific). Next, 400 ng of purified PCR product was used in an annealing reaction and enzymatic digestion by the T7E1 enzyme (New England Biolabs, Ipswich, MA, USA). The DNA fragments were separated on a 1.3% agarose gel and visualized by EB staining. The DNA band intensity was quantified using G:BOX (Syngene, Cambridge, UK) and analyzed with GelPro software (Media Cybernetics, Rockville, MD, USA). The INDEL frequency was estimated by comparing the digested band intensities to all bands.

The qEva-CRISPR assay generation

The qEva-CRISPR analysis was performed using the following custom-designed assays (probe mixes) with 7–12 MLPA probes: qEva_E4.1, qEva_E4.1_delA, qEva_E4.1_A/T, qEva_E4.2, qEva_HTT.sg1, qEva_HTT.sg3, qEva_HTT.sg4, qEva_HTT.edit, qEva_SNP, qEva_VEGFA, qEva_EMX1, qEva_CCR5.1, qEva_CCR5.6, qEva_CCR5.7 and qEva_multiplex. In most cases, the assay IDs corresponded to the IDs of the tested sgRNA/targets (Supplementary Table S2). Most assays consisted of one target specific (TS) probe and one to three off-target specific (OS) probes. The qEva_HTT.edit assay consisted of two probes (TS_HTT.sg1* and TS_HTT.sg4) specific for targets of HTT.sg1 and HTT.sg4 as well as one

probe (TS_HTT.HDR) specific for sequence overlapping the ssODN sequence (inserted to genome by HDR) and the genomic sequence flanking the incorporated ssODN sequence. Additionally, the 5′ half-probe of TS_HTT.sg1* and the 3′ half-probe of TS_HTT.sg4 formed a new probe (TS_HTT.sg1/4) that is specific to a new sequence created after rejoining of free-ends created after the excision of the sequence between the HTT.sg1 and HTT.sg4 cuts. In addition to the TS and OS probes, each assay consisted of up to eight control probes. The sequences, genomic positions, and detailed characteristics of the probes used in this study are presented in Supplementary Table S3. The qEva-CRISPR probes were designed according to a strategy previously proposed for MLPA probes (27,28). Three three-oligonucleotide probes (TS_HTT.HDR, TS_CCR5.1 and OS_CCR5.1) were designed according to a strategy adopted from (35,36). All probes were synthesized by IDT, Skokie, IL, USA. All reagents, except for the probe mixes, were purchased from MRC-Holland, Amsterdam, The Netherlands. The MLPA reactions were performed according to the manufacturer's general recommendations (http://www.mlpa.com). Briefly, 5 μl of genomic DNA (at a concentration of approximately 20 ng/μl) were incubated at 98°C for 5 min, cooled to room temperature and mixed with 1.5 μl of an appropriate probe mixture as well as 1.5 μl of SALSA hybridization buffer. The reaction was then denatured at 95°C for 2 min and hybridized at 60°C for 16 h. The hybridized probes were ligated at 54°C for 15 min by the addition of 32 μl of the ligation mixture. Following heat inactivation, the ligation reaction was cooled to room temperature, mixed with 10 μl of a PCR mixture (polymerase, dNTPs, and universal primers, one of which was labeled with fluorescein) and subjected to PCR amplification for 35 cycles.

The products of the MLPA reactions were diluted 20x in HiDi formamide containing GS Liz600, which was used as a DNA sizing standard, and separated via capillary electrophoresis (POP7 polymer) on an ABI Prism 3130XL apparatus (Applied Biosystems, Foster City, CA, USA). The obtained electropherograms were analyzed using GeneMarker software v2.4.0 (SoftGenetics, State College, PA, USA). The signal intensities (peak heights) were retrieved and transferred to prepared Excel sheets (available upon request). For each individual sample, the signal intensity of each probe was divided by the average signal intensity of the control probes to normalize the obtained values and to equalize the run-to-run variation. To calculate the relative signal (RS), the normalized signal of each probe was divided by the corresponding value of a reference (untreated) sample (or by the averaged value of the reference samples).

RESULTS

qEva-CRISPR strategy and assay design

For the proof-of-concept experiment, we designed two qEva-CRISPR assays (qEva_E4.1 and qEva_E4.2) specific to the INDEL scar-mutations generated by the well-validated E4.1 and E4.2 sgRNAs, which were developed previously (31). These sgRNAs target two non-overlapping sequences located in exon 4 of the *TP53* gene (Supplementary Table S2). Each of the assays included 8 control probes (specific to regions randomly distributed over the genome), one target-specific probe, and two (qEva_E4.1) or three (qEva_E4.2) off-target-specific probes. The off-target sequences, which were identified using Cas-OFFinder software (http://www.rgenome.net/cas-offinder/) (9), differed by 3–4 nucleotides from the corresponding target sequences (Supplementary Table S2). The set of control probes is universal and may be used in any qEva-CRISPR assay (except assays in which the control probes overlap with the tested target or off-target sites). The exact genomic location and sequence of each probe are indicated in Supplementary Table S3. The probes and general assay layouts were designed and generated according to a strategy developed for MLPA analysis that has been previously described in detail (27,28). We validated the performance of the assays with a panel of reference DNA samples and showed that each probe correctly recognized its target in the wild-type sequence [i.e. generates single PCR product (electropherogram peak) of the expected size].

qEva-CRISPR takes advantage of the fact that only perfectly hybridized MLPA half-probes can be ligated. Therefore, even a small mutation at the ligation point (predicted cut-site) prevents ligation and subsequent amplification of the probe. The amplification signal (amount of PCR product) is proportional to the dosage of matched (not-mutated) DNA molecules. Therefore, as shown in Figure 1A, the signal obtained for the target-specific probe in the DNA sample from cells treated with CRISPR/Cas9 reagents should be reduced proportionally to the fraction of mutated target sequences. In the case of modification of all targeted molecules, no signal of the target-specific probe should be present, whereas the signal for the control probes should remain intact (Figure 1A).

Using the developed assays, we analyzed HCT116 cells transfected with either the Cas9_E4.1 or Cas9_E4.2 plasmids. As shown in Figure 1B and Supplementary Figure S1, the relative signal (RS) of the target-specific probes decreased substantially in cells transfected with either of the plasmids. The level of the signal decrease corresponds to the fraction of modified target sequences expressed as the target modification efficiency (TME), which equals 49% (Supplementary Figure S1) and 43% (Figure 1B) for the E4.1 and E4.2 target sequences, respectively. In contrast, transfection with either of the plasmids did not affect the signals of off-target-specific probes (∼1, comparable to the signals of the control probes). This result indicated that with the conditions and sgRNAs that were used, the off-target sequences were not substantially edited. It must be noted; however, that some low-level (<5%) mutations in the tested regions may be missed. It results from the fact that to avoid false-positive detection of CRISPR/Cas9-induced mutations, signal changes smaller than 2 standard deviations (SDs) of the signals of control probes (usually smaller than 0.1 of RS or 10% of the TME value) were not considered significant.

Our experience, as well as the previous experiences of others, indicates that even the smallest mutation (mismatch of the probe with its target sequence) at the ligation point completely prevents ligation of the half-probes, which results in lack of signal for the affected probe [e.g. (27,37,38)]. To confirm this effect in our experimental system, we mod-

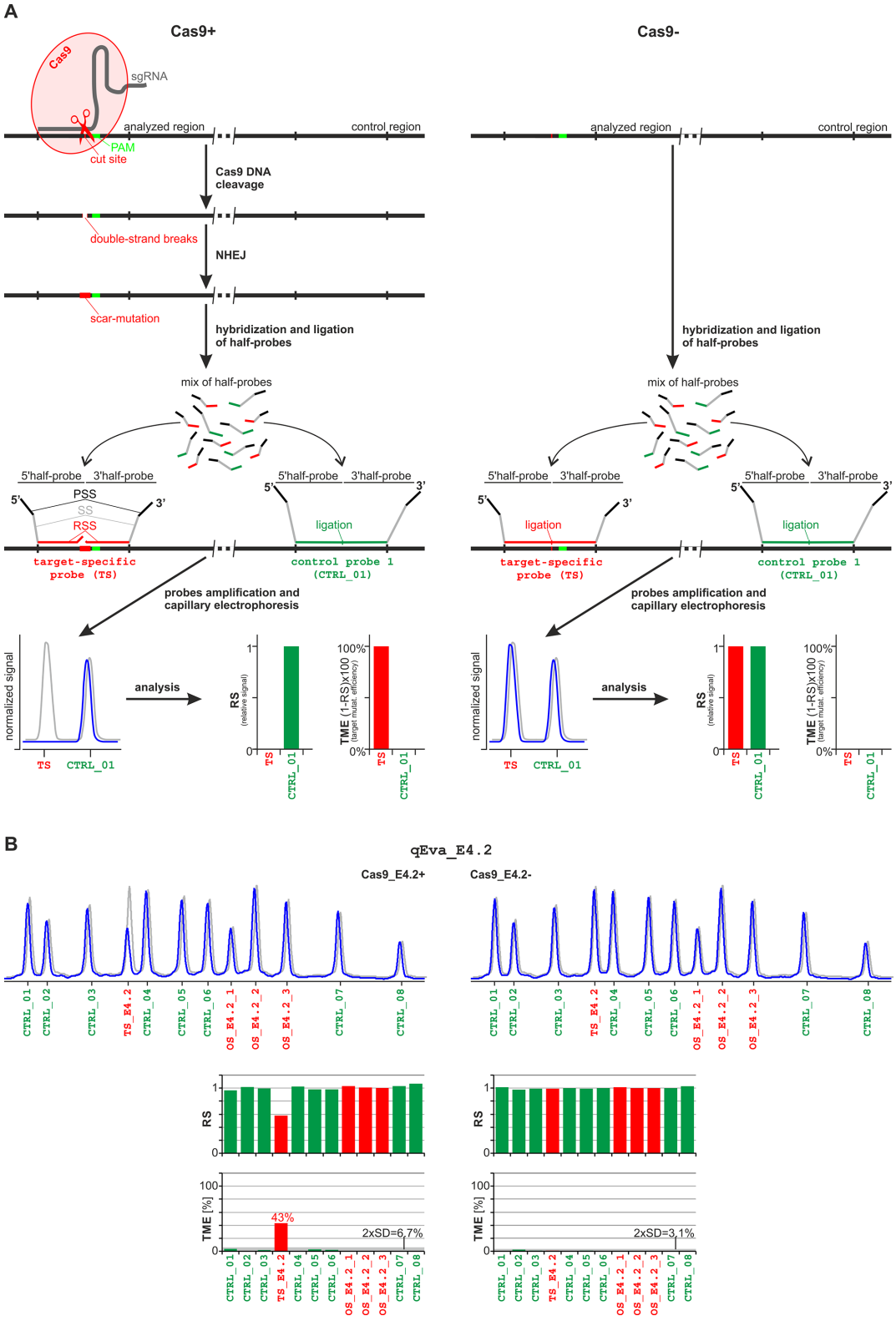

Figure 1. The qEva-CRISPR analysis strategy. (**A**) Schematic representation of qEva-CRISPR analysis of DNA samples extracted from cells either transfected (Cas9+; left-hand side) or not transfected (Cas9–; right-hand side) with a plasmid encoding CRISPR/Cas9 reagents. The Cas9 nuclease is directed toward target DNA by sgRNA, and after PAM recognition, DNA is specifically cleaved ~3-nt upstream of PAM. Double-strand breaks (DSBs) are mainly repaired by NHEJ, resulting in INDEL scar-mutations. Target and off-target-specific qEva-CRISPR half-probes are designed to directly adjust the predicted cut-sites. Therefore, the occurrence of any scar-mutation prevents ligation of sister half-probes and subsequent probe amplification. Each half-probe is composed of a region-specific sequence [RSS, indicated by either red (TS, target-specific probe) or green (CTRL, control probe)]; stuffer sequence (SS, gray), and primer-specific sequences [PSS, specific to either forward (fluorescently labeled) or reverse universal primers)]. Note that different lengths of

ified the target-specific probe TS_E4.1 by introducing either a single substitution or single-nucleotide deletion into one of its half-probes (for details, see Supplementary Table S3 and Supplementary Figure S2). As shown in Supplementary Figure S2, any of the single-nucleotide mutations caused complete reduction of probe signal (i.e., no detectable signal in the expected position).

In addition, we designed an assay (qEva_SNP) specific for three different SNPs that served as a model for very small [single-nucleotide (sn) substitution, sn deletion, and sn insertion] CRISPR/Cas9-induced alterations. As shown in Supplementary Figure S3, qEva-CRISPR was able to specifically and quantitatively recognize all nucleotide alterations. The experiment confirmed that even small alteration at the ligation point prevents any signal of qEva-CRISPR probes. The experiment also confirmed the multiplexing capability of qEva-CRISPR. Further, to test the sensitivity and threshold of qEva-CRISPR mutation detection, we performed a titration experiment with decreasing amounts of sample containing the selected SNPs. As shown in Supplementary Figure S3B, the signal of a particular alteration still may be detected even if it is present in low fraction (∼2%). However, mutations detected at a very low level (<5%) should be interpreted carefully (which applies to most other methods as well).

Analysis of the well-characterized *VEGFA*, *CCR5* and *EMX1* sgRNAs activity with qEva-CRISPR

To demonstrate the utility and robustness of qEva-CRISPR for a wider range of targets, we designed five new assays that were specific for 5 different targets and corresponding off-targets, i.e. sgRNAs for *VEGFA* and *EMX1* and three sgRNAs for *CCR5*. The CRISPR/Cas9 activity towards the selected targets was analyzed before by T7E1 and NGS (33,39,40). As shown in Supplementary Figure S4A–C, the designed assay detected different levels of modification of target and off-target sites that generally corresponded to the results of previous studies (33,39,40). Please note that some of the targets (*CCR5*) are segmentally duplicated in other parts of the genome, which creates highly similar sequences (off-targets) (Supplementary Table S2). The high similarity of these sequences results in almost identical editing efficiency of the *CCR5* targets and the corresponding off-targets. A similar effect was also observed for the *EMX1* target but not for the *VEGFA* target, which differed more substantially from the off-target (compare Supplementary Figure S4 and Supplementary Table S2). To demonstrate the multiplexing ability of qEva-CRISPR, we designed an assay (qEva_multiplex) for parallel analysis of 3 targets (VEGFA, EMX1, and CCR5.7). We used qEva_multiplex for analysis of K562 cells, which were simultaneously transfected with three plasmids encoded the corresponding sgRNAs. (Supplementary Figure S4D).

Evaluation of experimental conditions that affect genome editing

To determine how the concentration of the plasmid encoding CRISPR/Cas9 components affects the efficiency of the target mutation, we transfected HCT116 and HeLa cells with increasing amounts (0.25–2 μg) of the Cas9_E4.1 and Cas9_E4.2 plasmids. As shown in Figure 2A, the fractions of the modified target sequences gradually increased from ∼0% at the lowest concentration to ∼35% at the highest concentration of plasmid. The efficiency of the target modification was comparable for the Cas9_E4.1 and Cas9_E4.2 plasmids in both HCT116 and HeLa cells. The signal of the off-target probes remained unchanged regardless of the concentration of plasmid and the type of transfected cells. The obtained qEva-CRISPR results corresponded well to the fraction of transfected cells observed using fluorescence microscopy (Figure 2A, insets) and correlated well (R^2 = 0.88–0.99) with the fraction of GFP-positive cells counted using flow cytometry (Figure 2B). It must be stressed, however, that the obtained results are specific to the experimental conditions and cannot be generalized to other sgRNAs or cell types.

In the next step, we analyzed the efficiency of the target modification in GFP-positive HCT116 cells fractionated by flow cytometry into three groups with high, medium, and low GFP fluorescence intensity. The experiment was performed with cells that were either transfected (Lipofectamine LTX) or electroporated with the Cas9_E4.2 plasmid. As shown in Figure 3, the efficiency of the target modification differed slightly depending on the method of transfection (i.e. higher for electroporation than lipofection). As expected, TME was generally higher in the fraction of GFP-positive cells than in unsorted cells (for comparison, see Figure 2; for cell-sorting parameters, see Supplementary Figure S5). The results are generally consistent with the efficiency of the target modification evaluated using the method based on T7E1 heteroduplex cleavage (Figure 3B).

Targeted gene modification in single-cell-derived clones

In the next step, we analyzed the level of target modification in single-cell-derived clones of HCT116 cells trans-

←

SSs allow for probes length differentiation and their separation by capillary electrophoresis. The signals of all of the probes were normalized (divided) to the average signal of the control probes (CTRL) and then to calculate the relative signal (RS) compared with the corresponding signals in a reference (untreated) sample. The signals of each probe are presented as bar plots, either as the RS or percent of the target mutation efficiency (TME = (1 – RS) × 100%). (**B**) Analysis of the target (*TP53*) and off-target mutation efficiencies in HCT116 cells either transfected (1.5 μg of plasmid DNA) or not transfected with the Cas9_E4.2 plasmid. From the top: overlapped electropherograms of the analyzed (blue) and reference (gray) samples, corresponding RS, and TME bar plots. The electropherograms were generated using the GeneMarker program (SoftGenetics, State College, PA) and captured as screenshots. The electropherogram lines were then extracted from the screenshot-bitmaps using the 'Trace line' tool in Corel Graphic v.X8. The probe IDs (TS – target-specific probe; OS – off-target-specific probes, CTRL – control probes) are indicated under the electropherograms and under the bar plots. The gray zone in the TME graphs indicates the significance threshold, 2× the standard deviation (SD) of the control probes signals. Target and off-target probes are indicated in red; control probes are indicated in green. The decrease in the signal of the TS probe corresponded to a TME of 43%, whereas the signal from two off-target specific probes remained unchanged (no mutation was detected). Corresponding results for the Cas9_E4.1 plasmid are shown in Supplementary Figure S1.

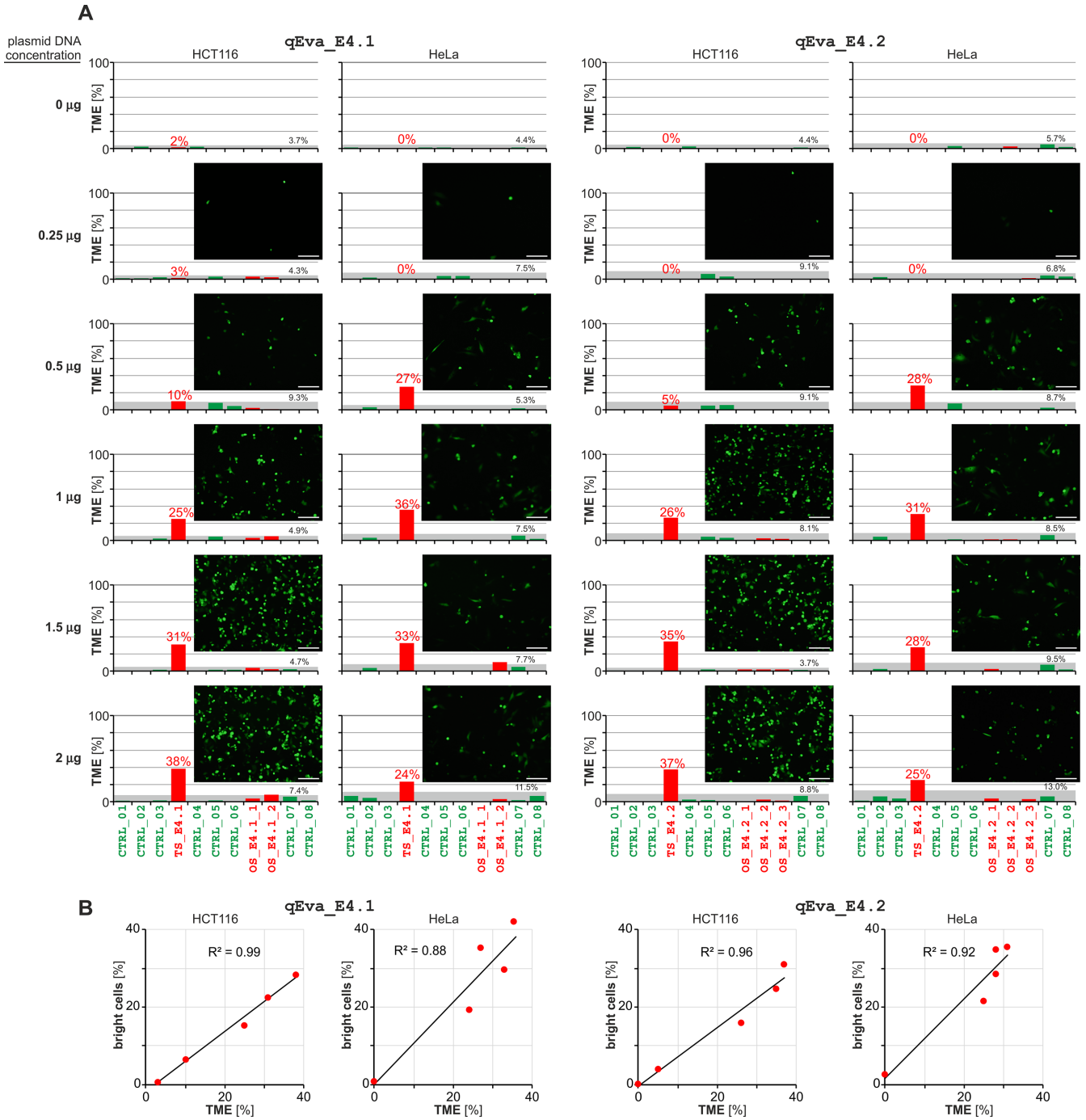

Figure 2. Effects of plasmid concentration on the efficiency of Cas9-induced target modification. (**A**) TME bar plots depicting the results of qEva-CRISPR analysis of HCT116 and HeLa cells transfected with increasing concentrations of either Cas9_E4.1 (left-hand side) or Cas9_E4.2 (right-hand side) plasmids. The chart designations are as shown in Figure 1B. The insets in each graph depict representative images of transfected cells (green fluorescent spots) expressing GFP as a marker. Scale bars, 50 µm. (**B**) Correlation of the TME values (x-axis) determined by qEva-CRISPR analysis (above) with the percentage of GFP-positive cells (y-axis) observed after plasmid transfection. GFP signals were detected in FL1 with the standard BD Accuri C6 filter configuration FL1 = 533/30 nm. Gates were set based on the untransfected controls.

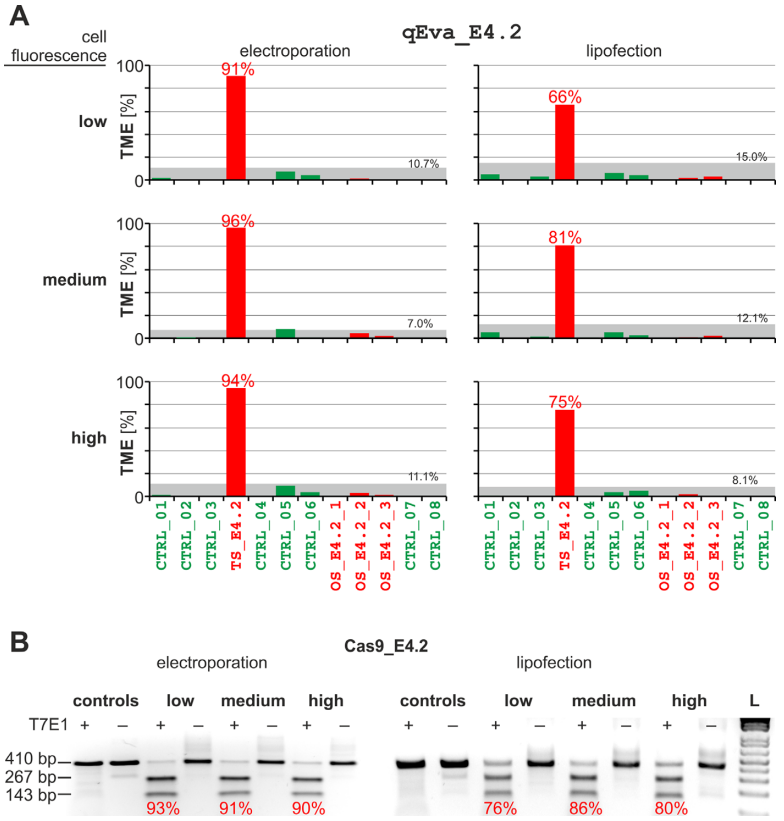

Figure 3. Analysis of the Cas9-induced target modification efficiency in GFP-positive cells. The GFP signal indicates cells carrying the Cas9_E4.2 plasmid transfected either by electroporation (left-hand side) or lipofection (right-hand side). Based on the fluorescence intensity, GFP-positive cells were divided into three arbitrarily designated categories: low, medium, and high. (**A**) The TME bar plots depicting the results of qEva-CRISPR analysis of low, medium, and high fractions of the HCT116 GFP-positive cells. The chart designations are as shown in Figure 1B. (**B**) Agarose gels depicting the results of T7 endonuclease I (T7E1) analysis of DNA samples from the above-described cells. Bands representing full-length (410 bp) and digested PCR products (~267 bp and 143 bp) are indicated on the left. Only heteroduplexes with Cas9-induced mismatches are digested by T7E1. PCR products digested (+) and not digested (–) with T7E1 are shown next to each other. Control – PCR product of DNA samples extracted from cells not transfected with Cas9_E4.2 plasmid; L – 1 Kb Plus DNA ladder (ThermoFisher Scientific, Waltham, MA). The percentage of digested products (calculated based on the densitometric analysis) corresponding to a fraction of the Cas9-mutated targets are shown in the particular lines on agarose gels (red fonts).

fected with either Cas9_E4.1 or Cas9_E4.2 plasmids. As shown in Figure 4A, the level of target modification in both cases was either close to 0% or close to 100%, which suggested that either no allele was mutated or both alleles of the analyzed cells were mutated. There were no intermediate values (close to 50%) that would indicate mutation of just one allele (heterozygous mutation). The results of the Sanger sequencing analysis of selected clones were perfectly consistent with the observed genotypes (which confirm either wild-type or biallelic mutations) (Figure 4B). In contrast, the levels of off-target mutations were consistently close to 0%, which indicates there was no mutation of the analyzed off-targets in the tested clones. It must be noted, however, that in some clones with biallelic mutations, the signal of the target-specific probes was not completely reduced (RS > 0), and it corresponds to TME values close but not equal to 100% (Figure 4A). The occurrence of some signal of target-specific probes in single-cell-derived clones with biallelic mutations may result either from some contamination of the analyzed clone with wild-type cells (clone cross-contamination) or from the occurrence of a mutation that allows for some low-level hybridization and subsequent ligation of the probe. The second explanation seems to be less likely (see Supplementary Figure S2).

Application of qEva-CRISPR for analysis of 'difficult' genomic regions

We tested the applicability of qEva-CRISPR for analysis of 'difficult' regions enriched in low complexity and highly repetitive sequences. Such regions are generally very difficult or not possible to analyze using standard genetic approaches. For this purpose, we designed three qEva-CRISPR assays (i.e. qEva_HTT_sg1, qEva_HTT_sg3, and qEva_HTT_sg4) to analyze the targets located in exon 1 of the *HTT* gene in close proximity to polymorphic microsatellite tracts (CAG and CCG) (Figure 5A and B), the expansion of one of which (CAG) causes Huntington's disease. These assays utilized a set of previously designed control probes. As shown in Figure 5B, some half-probes of the target-specific probes showed substantial overlap with highly redundant repetitive sequences. The specificity of these probes was guaranteed by combination with a second, more specific half-probe. The experiment performed in four biological replicates, clearly showed that each of the applied

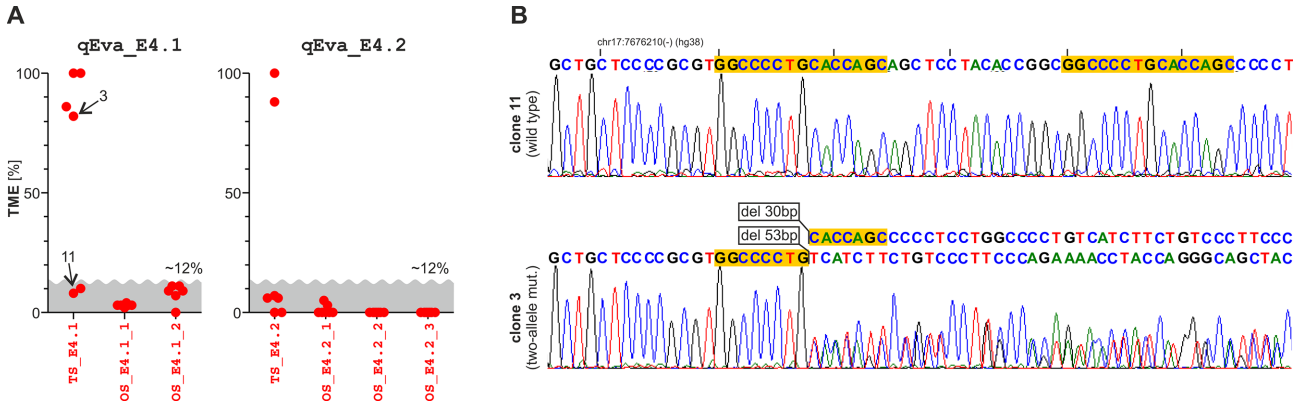

Figure 4. Analysis of the level of target modifications in single-cell-derived clones of HCT116 cells transfected with either Cas9_E4.1 or Cas9_E4.2 plasmids. (**A**) A dot-plot depicting the TME values of target- and off-target-specific probes. Each dot represents the TME value of one analyzed clone. The gray zone indicates the approximate level of 2x the SD observed in the analyzed clone samples. (**B**) Sanger sequencing analysis of the Cas9_E4.1 target site in clone 11 with the wild-type sequence and clone 3 with biallelic deletions in the target sites. The dots representing clone 3 and clone 11 are indicated in the dot-plot presented in panel A. Yellow backgrounds indicate micro-homologous sequences flanking the Cas9_E4.1 target site.

sgRNAs efficiently induced mutations in the corresponding target with HTT.sg4 showing the highest efficiency (Figure 5C and D). The tested off-targets of the HTT.sg3 and HTT.sg4 sgRNAs were not affected. In contrast, both of the tested off-targets (HTT.sg1_1 and HTT.sg1_2) of the HTT.sg1 sgRNA were substantially modified (Figure 5C and D). The high mutation rate of these off-targets was consistent with their high similarity to the target (single mismatch at the second nucleotide upstream of the expected cut-site) (Supplementary Table S2). For comparison to biological variation (Figure 5D), we performed technical replication (7×) of the selected experiment as well. As shown in our results (compare Figure 5D and E), the technical variation is very small, and therefore, most qEva-CRISPR variability results from biological components. Additionally, we replicated analysis of HTT.sg1 efficiency with the use of a ribonucleoprotein (RNP) complex delivery system. This dose-dependent experiment was performed in HEK293 cells with four biological replicates (Figure 5F). As shown in our results, the RNP delivery system generally resulted in lower target modification efficiency, but it also resulted in substantially lower modification of the off-targets.

Distinguishing HDR from NHEJ

Finally, we designed the qEva_HTT.edit assay to demonstrate that qEva-CRISPR can be applied not only to analyze the level of 'destruction' of specific sequences (loss of signal by Cas9 cutting) but also to detect and quantify new sequences (gain of signal) generated by NHEJ or HDR. In the first step, we used previously described HTT.sg1 and HTT.sg4 for precise excision of the DNA sequence between cuts generated by either Cas9 or Cas9n (34). As shown in Figure 6A–B, excision of the DNA fragment resulted in a decrease in the signal of the HTT.sg1 and HTT.sg4-specific probes. Simultaneously, the signal of the TS_HTT.sg1 /4 probe appears. The results indicate clean rejoining of the DNA free-ends by NHEJ. In addition, to demonstrate detection of new sequences introduced by HDR, we transfected HEK293T cells with Cas9(n)_HTT.sg1 and Cas9(n)_HTT.sg4 plasmids along with the donor template (ssODN containing fragment of GFP sequence). As shown in Figure 6C, qEva-CRISPR can detect and distinguish new sequences created either by NHEJ (with clean ends rejoining) or HDR. Analysis of single-cell-derived clones confirmed the ability of qEva-CRISPR to detect specific sequences resulting from various repair mechanisms (Figure 6D and E).

DISCUSSION

New CRISPR technologies for targeted genome editing are still being developed, which will enhance the range of applications and possible targets. A simple method for reliable and quantitative determination of INDEL mutations in a target sequence is important for the selection of effective approaches and CRISPR reagents, including targeting sgRNAs. Another important factor that requires careful evaluation is the specificity of the approach that is used, which is especially important for therapeutic applications and preclinical studies.

The typical result of the genome editing procedure is a heterogeneous mixture of different types of mutations occurring at a target site that is additionally accompanied by an unmodified wild-type target sequence. This heterogeneity substantially hampers reliable evaluation of editing efficiency, especially for quantification. The methods that allow for detection and quantification of CRISPR-induced mutations include NGS [e.g., (39)]; Tracking of Indels by DEcomposition (TIDE) [(21,22)]; Indel Detection by Amplicon Analysis (IDAA) (41); and the Droplet Digital PCR (ddPCR)-based method (42).

The advantage of NGS, especially whole-genome NGS, is its ability to detect the CRISPR-induced mutation in any region of the genome, not only mutations occurring in a predefined target or off-targets but also accidental mutations in regions that are difficult or impossible to predict. This characteristic makes NGS a method of choice for the final verification of editing outcomes, especially when it is used in the context of clinical applications. On the other hand, NGS is still costly, cumbersome and time-consuming (NGS library

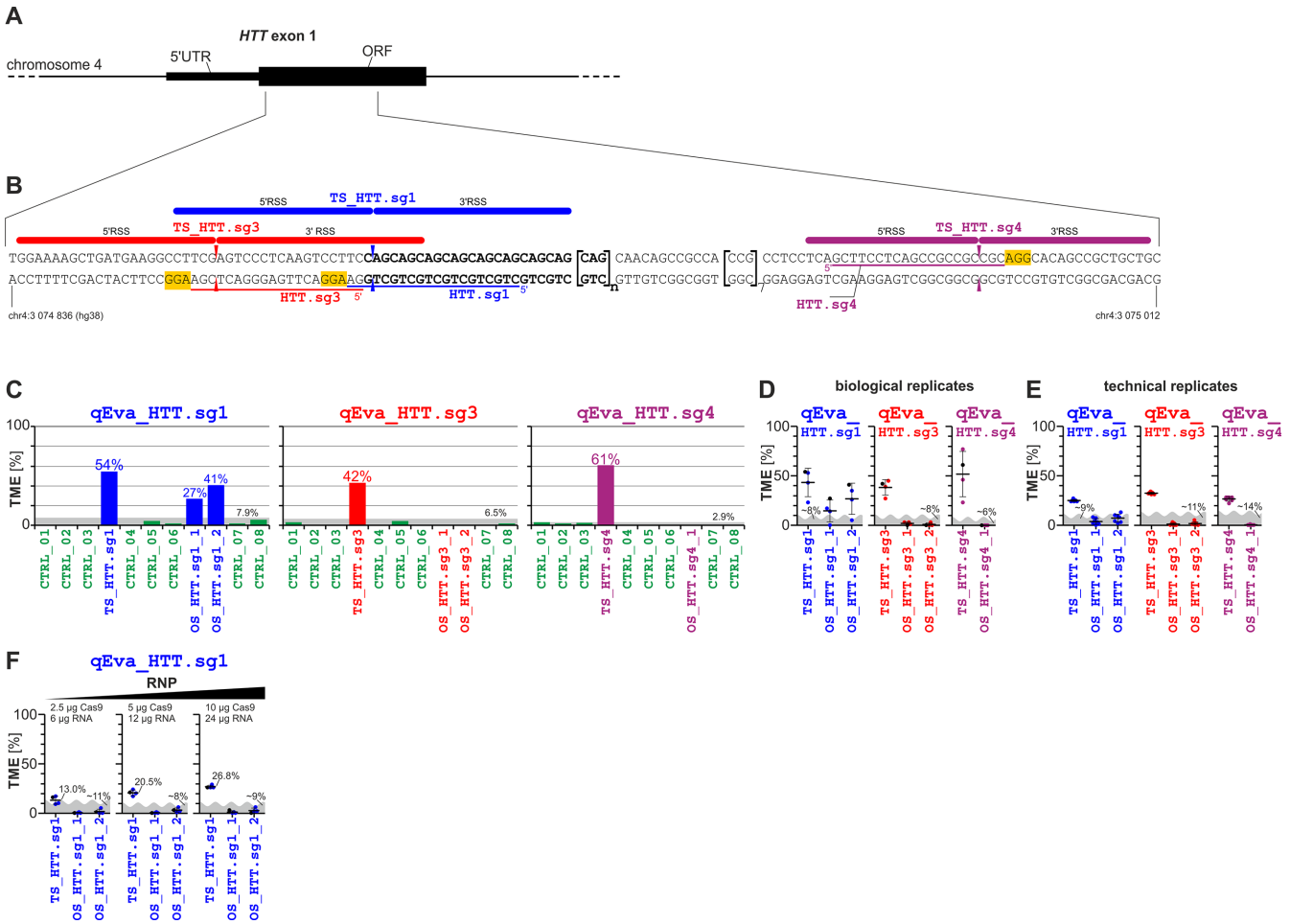

Figure 5. Assay design and analysis of the Cas9-induced target modification efficiency in the region of the *HTT* gene. (**A**) Schematic representation of exon 1 of the *HTT* gene with lower and higher rectangles representing the 5′UTR and coding sequence, respectively. (**B**) The sequence of *HTT* exon 1 with the indicated target sequences (thin lines below the targeted strand), corresponding to predicted cut-sites (arrowheads) and PAMs (yellow background). The 5′ and 3′ RSSs of the qEva-CRISPR probes specific to particular target sites are depicted above the sequence. Bold font indicates a CAG repeat sequence, which can lead to Huntington's disease if repeats are expanded. Please also note the presence of other repetitive and low-complexity elements in the sequence (e.g. CCG repeats). (**C**) The TME bar graphs depicts the level of the target and corresponding off-target modifications in the transfected HEK293T cells. Blue, red, and purple colors indicate the HTT.sg1, HTT.sg3 and HTT.sg4 target sequences as well as the corresponding qEva-CRISPR probes and target/off-target-specific bars in the TME graph, respectively. (**D**) Dot-plots summarizing results (TME values in the tested target/off-target sites) of four independent CRISPR/Cas9 experiments (biological replicates). Dots represent the TME values of individual experiments (black dots indicate the results shown in (C), horizontal lines represent the medians, and whiskers represent the SD values. (**E**) Dot plots summarizing the results (TME values in the tested target/off-target sites) of seven qEva-CRISPR analyses (technical replicates) for the same CRISPR/Cas9 experiment. The graphs scheme as shown in (D). (**F**) The results of four independent experiments of CRISPR/Cas9-induced sequence modifications performed with the use of HTT.sg1 delivered in increasing amounts (indicated over the graphs) of RNP complex. The dot plots scheme is the same as shown in (D), blue and black dots represent experiments performed in the HEK293T and GM04281 cells, respectively.

preparation and data analysis), and it is often performed with the use of an external service. Therefore, NGS is impractical and rarely used in everyday laboratory work. The methods that may overcome this gap are the TIDE, IDAA and ddPCR-based methods as well as qEva-CRISPR. All of these methods have a similar cost (~$10 per sample; depending on the analysis setup) and require a similar amount of time for analysis (1–2 days). All of them need only basic and easily accessible laboratory equipment, such as a thermocycler and either a CE-apparatus (TIDE, IDAA, qEva-CRISPR) or ddPCR equipment dedicated to droplet generation and counting. The TIDE method is based on the decomposition of Sanger sequencing traces to identify major mutations induced in the expected editing sites. The main advantage of TIDE is that it simultaneously identifies and quantifies all major mutations occurring at the target site. It was shown that TIDE results excellently correlate (predict) with the global effects of target modification. However, the estimated level of individual mutations may deviate from expected (from replicate or control experiments) by a few percentage points, and it is somehow less reliable for mutations occurring at a low frequency as well as for larger INDELs. Inherently, the reliability of TIDE depends on the purity/quality of PCR products and Sanger sequencing reads, and therefore, sequencing the opposite strand to confirm the results is recommended. IDAA is a very simple and straightforward method that takes advantage of the high resolution (1 nt) of capillary electrophoresis for sepa-

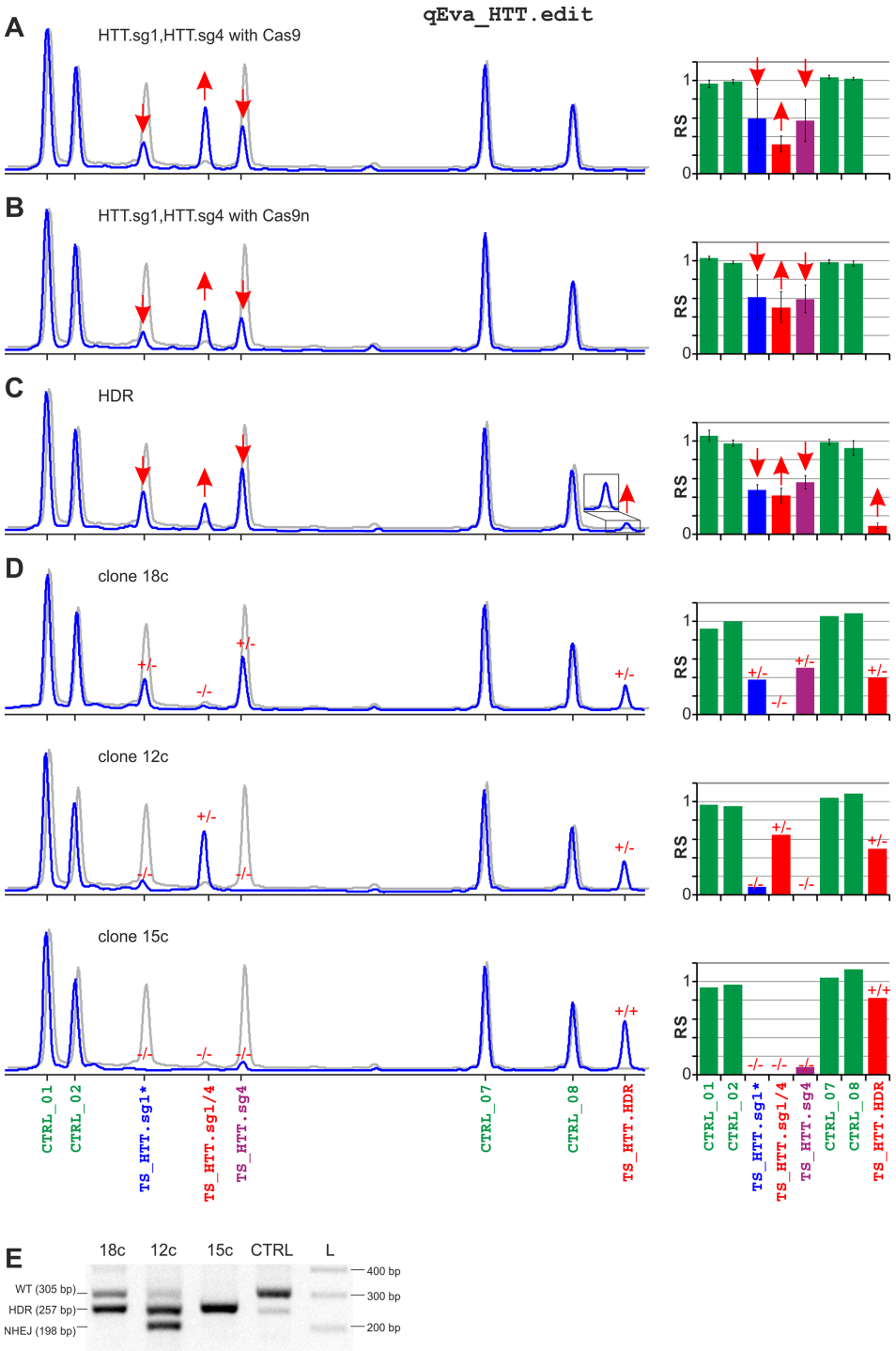

Figure 6. Analysis of NHEJ and HDR events after targeted editing of the *HTT* gene by CRISPR/Cas9. (**A**) Results of the HTT gene editing with the use of two sgRNAs (HTT.sg1 and HTT.sg4, as shown in Figure 5) flanking the (CAG)n repeat tract; (left-hand-side) electropherograms of the qEva_HTTedit assay of treated (blue) versus untreated (reference; gray) samples; (right-hand-side) RS-bar plot summarizing the results of 3 independent experiments (error bars indicate SD). Note that the excision of a genomic fragment between the HTT.sg1 and HTT.sg4 cuts destroys both targets and decreases the signal of both target-specific probes. Subsequent rejoining of the free-ends by NHEJ creates a new sequence that is recognized by the TS_HTT.sg1/4 probe that is composed of the 5′ half probe of TS_HTT.sg1* and the 3′half probe of TS_HTT.sg4 (see Supplementary Table S3). The signal of TS_HTT.sg1/4 is not present in a reference sample and increases after the treatment. (**B**) Similar to (A) but conducted with Cas9n (instead of Cas9). (**C**) Similar to (A) but conducted with an ssODN composed of a 59-nt insert sequence and 60-nt 5′ and 3′ arms homologous to the HTT.sg1 and HTT.sg4 flanks. The appearance of the HTT_HDR probe signal indicates the successful introduction of the insert by HDR. (**D**) Examples of single-cell-derived clones generated from the experiment as shown in (C): (from the top) the clone with one allele with wild-type sequence and one allele modified by HDR; one allele modified by HDR and the other by NHEJ; and the clone with two alleles modified by HDR. (E) The agarose gel analysis of the clones shown in (C) (clone IDs are shown above the gel). The PCR product was generated with primers flanking the modification site. WT – the PCR product of wild-type sequence; HDR – the product of sequence repaired by HDR; and NHEJ – the product of sequence repaired by NHEJ (with clean ends rejoining).

ration of all INDEL mutations. Its limitation, however, is that it cannot detect substitutions, which means that it (in contrast to TIDE and qEva-CRISPR) cannot be used for analysis of the efficiency of recently developed strategies of targeted base editing [e.g. (43) and references within]. Similar to TIDE and other PCR-based methods (unlike qEva-CRISPR) IDAA does not allow for detection of larger rearrangements extending beyond amplicon size. Additionally, IDAA relies on the analysis of a homogenous PCR product. Therefore (like TIDE), it is less suitable for regions with overlapping tandem repeats and INDEL polymorphisms. A recent direct comparison of T7E1, TIDE and IDAA with NGS used as a gold standard showed that both TIDE and IDAA substantially outperform T7E1 that turned out to poorly predict editing efficiency (44). The results also showed that both TIDE and IDAA overestimate (10–20%) the presence of wild-type sequences and miscall some mutations, especially 'complex' ones. Despite their specific limitations, both TIDE and IDAA are presently methods of choice for standard analysis of genome editing. However, both methods are less suitable for analysis of targets located in 'difficult regions' and they have little potential for multiplexing.

More recently, two strategies (based on similar principles) of genome editing evaluation that take advantage of the partitioned amplification of individual copies of DNA with the use of ddPCR have been proposed (42,45). The ddPCR-based method utilizes two fluorescently labeled probes that are specific for closely located sequences (one close to the wild-type reference site and the other close to the expected target-cut-site). The absolute quantification of PCR droplets positive for one and two probes allows for evaluation of the fraction of edited DNA molecules. The ddPCR-based method potentially allows for detection of a very small fraction of mutated molecules. However, the performance of this method strongly depends on assay conditions and the amount of DNA used for analysis (both factors require optimization and may affect the precision of analysis) (Findlay SD). It may be expected that improvement of ddPCR technology (both in terms of a number of analyzed droplets and assay conditions) may further enhance the sensitivity and reliability of the ddPCR-based method and make it a method of choice to detect mutations present in a very small fraction of analyzed molecules.

The main advantages of qEva-CRISPR compared to these methods include multiplexing, its relative insensitivity to mutation type, the capability for analyzing targets located in 'difficult regions' and for distinguishing HDR and NHEJ. We tested the qEva-CRISPR strategy and confirmed its reliability using ten CRISPR/Cas9 targets located in the *TP53, VEGFA*, *EMX1* and *CCR5* genes as well as the highly repetitive region of the *HTT* gene. Reliable analysis of Cas9-mediated mutations in the latter region was not possible using other PCR-based or sequencing-based methods. The designed qEva-CRISPR assays were tested in four different cell types under numerous experimental conditions and designs (i.e. different plasmid and RNP concentrations, transfection methods, sorted and unsorted cells, and single-cell-derived clones) as well as artificial models. To test the reliability of qEva-CRISPR, we compared the obtained results with (i) the number of positively transfected (GFP-positive) cells observed either with fluorescence microscopy or counted with a flow cytometer, (ii) the results obtained for T7E1 analysis, (iii) Sanger sequencing of the target sequences in single-cell-derived clones and (iv) the results of previous studies. All of the performed analyses showed substantial consistency with the qEva-CRISPR results.

The target-specific qEva-CRISPR probes were designed to overlap target sequences with the ligation position located directly over the predicted cut-sites (Figure 1A, also B), which makes them (and qEva-CRISPR analysis) sensitive to any type of mutation occurring at the target sites, including both small mutations (even single-nucleotide substitutions or deletions) and large deletions or more complex rearrangements. It has been previously shown [e.g. (27,37,38)] and confirmed herein (Supplementary Figure S2 and Supplementary Figure S3) that even a small mismatch at the ligation point completely prevents ligation and subsequent amplification of the probe. It was also shown that the signal of the MLPA probes is quantitatively proportional to the dosage (number of copies) of the tested regions [e.g. (46–48)]. Sensitivity to large deletions is the main property of the ligation-dependent probes that are routinely utilized in MLPA assays for large mutation detection [e.g. (27,29,49,50)]. Moreover, the short region-specific sequence (usually ∼40 nt) of the qEva-CRISPR probes utilized in our study made them relatively insensitive to the single-nucleotide substitutions (SNPs) that commonly occur in the human genome as well as in other genomes. Because the most common SNPs in the human genome have already been identified and deposited in the appropriate databases (e.g. dbSNP), qEva-CRISPR probes may, in most cases, be designed to avoid common SNPs in a relatively short region-specific sequence [see protocol in (28)]. The occurrence of SNPs is a serious drawback of all heteroduplex-based methods, which usually use relatively long PCR amplicons (∼400 nt) that often overlap with common SNPs and interfere with subsequent analyses.

The experiments that were performed also confirmed that qEva-CRISPR analysis may be used for optimization and selection of the best experimental conditions (plasmid and RNP concentration or transfection method) for most effective target modifications or for the selection of single-cell-derived clones with the desired genotype, including specific genotypes generated by HDR or NHEJ without the need for cumbersome and time-consuming cloning and sequencing of individually targeted alleles.

The advantages of our qEva-CRISPR assays are as follows. (i) qEva-CRISPR is a multiplex method that enables simultaneous analysis of target and off-target regions. In the same way, it could be adapted for simultaneous analysis of more than one target site. (ii) qEva-CRISPR is a semi-quantitative method that allows for robust estimation of the fraction of modified targets. (iii) qEva-CRISPR may be designed to detect and distinguish new sequences generated by NHEJ and HDR. (iv) The sensitivity of qEva-CRISPR does not depend on the mutation type. The qEva-CRISPR probe may detect both single-nucleotide substitutions and deletion of the whole gene. (v) qEva-CRISPR allows for detection of homozygous mutations without the need for the addition of wild-type DNA, which is required in all methods that rely on heteroduplex formation. (vi) qEva-

CRISPR does not require the optimization and adjustment of assays for the specific target sequence. It takes advantage of a standard protocol (standard reaction conditions, easily accessible reagent set) of MLPA. The standard MLPA setup was validated and successfully used in hundreds of research and clinical studies for the analysis of large mutations in disease-related genes [e.g. (27,29,49,50)]. (vii) The qEva-CRISPR strategy can be easily adapted to the target or off-targets of interest. This approach requires only the design of target-specific probes that may be used together with a set of control probes designed for this study (upon request, we may share aliquots of a ready-to-use mix of control probes). (viii) The qEva-CRISPR test is cost-effective (∼$10 per sample, including the reagents and cost of the capillary electrophoresis separation (excluding the starting cost of probes synthesis, which is ∼$150 per probe, the synthesized probe may be used for thousands of reactions). (ix) qEva-CRISPR does not require advanced laboratory equipment. (x) Finally, due to the characteristics of the target-specific probes and the strategy utilized for the probe design [described in detail previously by our group (27,28)], qEva-CRISPR may be used to analyze almost any target or targets of interest, including targets located in 'difficult' genomic regions.

It must also be noted that qEva-CRISPR has limitations. It cannot be used for a whole-genome analysis and does not allow for detection of all potential and accidental off-target sites, and it generally does not characterize the identified mutations. qEva-CRISPR does not allow for reliable detection of a mutation that occurs in a very small fraction (∼5%) of targets. However, because in most experiments, only results in which the target of interest is substantially modified are considered important and worthy of further analysis, the latter drawback has a limited impact on this method.

In summary, the plethora of methods developed for evaluating genome editing efficiency (including methods not discussed here) indicates there is no ideal method that fulfills all requirements for testing the efficiency. The methods discussed in this study have different advantages and are optimal for different applications. We may expect that in the future, either one method will turn out to be superior and will dominate the others or, more likely, different methods will form niches for specific applications.

SUPPLEMENTARY DATA

Supplementary Data are available at NAR Online.

FUNDING

National Science Center PL [2015/18/E/NZ2/00678 and 2016/22/A/NZ2/00184]; Ministry of Science and Higher Education PL [KNOW program for years 2014–2018]. Funding for open access charge: National Science Center [2015/18/E/NZ2/00678].
Conflict of interest statement. None declared.

REFERENCES

1. Jinek,M., Chylinski,K., Fonfara,I., Hauer,M., Doudna,J.A. and Charpentier,E. (2012) A Programmable Dual-RNA-Guided DNA endonuclease in adaptive bacterial immunity. *Science*, **337**, 816–821.
2. Ran,F.A., Hsu,P.D., Wright,J., Agarwala,V., Scott,D.A. and Zhang,F. (2013) Genome engineering using the CRISPR-Cas9 system. *Nat. Protoc.*, **8**, 2281–2308.
3. Mojica,F.J.M., Diez-Villasenor,C., Garcia-Martinez,J. and Almendros,C. (2009) Short motif sequences determine the targets of the prokaryotic CRISPR defence system. *Microbiology*, **155**, 733–740.
4. Anders,C., Niewoehner,O., Duerst,A. and Jinek,M. (2014) Structural basis of PAM-dependent target DNA recognition by the Cas9 endonuclease. *Nature*, **513**, 569–573.
5. Urnov,F.D., Miller,J.C., Lee,Y.L., Beausejour,C.M., Rock,J.M., Augustus,S., Jamieson,A.C., Porteus,M.H., Gregory,P.D. and Holmes,M.C. (2005) Highly efficient endogenous human gene correction using designed zinc-finger nucleases. *Nature*, **435**, 646–651.
6. Dahlem,T.J., Hoshijima,K., Jurynec,M.J., Gunther,D., Starker,C.G., Locke,A.S., Weis,A.M., Voytas,D.F. and Grunwald,D.J. (2012) Simple methods for generating and detecting Locus-Specific mutations induced with TALENs in the zebrafish genome. *PLoS Genet.*, **8**, e1002861.
7. Jiang,F.G. and Doudna,J.A. (2017) CRISPR-Cas9 structures and mechanisms. *Annu. Rev. Biophys.*, **46**, 505–529.
8. Moreno-Mateos,M.A., Vejnar,C.E., Beaudoin,J.D., Fernandez,J.P., Mis,E.K., Khokha,M.K. and Giraldez,A.J. (2015) CRISPRscan: designing highly efficient sgRNAs for CRISPR-Cas9 targeting in vivo. *Nat. Methods*, **12**, 982–988.
9. Bae,S., Park,J. and Kim,J.S. (2014) Cas-OFFinder: a fast and versatile algorithm that searches for potential off-target sites of Cas9 RNA-guided endonucleases. *Bioinformatics*, **30**, 1473–1475.
10. Erard,N., Knott,S.R.V. and Hannon,G.J. (2017) A CRISPR resource for individual, combinatorial, or multiplexed gene knockout. *Mol. Cell*, **67**, 348–354.
11. Tsai,S.Q. and Joung,J.K. (2016) Defining and improving the genome-wide specificities of CRISPR-Cas9 nucleases. *Nat. Rev. Genet.*, **17**, 300–312.
12. Zischewski,J., Fischer,R. and Bortesi,L. (2017) Detection of on-target and off-target mutations generated by CRISPR/Cas9 and other sequence-specific nucleases. *Biotechnol. Adv.*, **35**, 95–104.
13. Kim,Y., Kweon,J., Kim,A., Chon,J.K., Yoo,J.Y., Kim,H.J., Kim,S., Lee,C., Jeong,E., Chung,E. *et al.* (2013) A library of TAL effector nucleases spanning the human genome. *Nat. Biotechnol.*, **31**, 251–258.
14. Qiu,P., Shandilya,H., D'Alessio,J.M., O'Connor,K., Durocher,J. and Gerard,G.F. (2004) Mutation detection using Surveyor nuclease. *Biotechniques*, **36**, 702–707.
15. Zhu,X.X., Xu,Y.J., Yu,S.S., Lu,L., Ding,M.Q., Cheng,J., Song,G.X., Gao,X., Yao,L.M., Fan,D.D. *et al.* (2014) An efficient genotyping method for Genome-modified animals and human cells generated with CRISPR/Cas9 system. *Sci. Rep.*, **4**, 6420.
16. Vouillot,L., Thelie,A. and Pollet,N. (2015) Comparison of T7E1 and surveyor mismatch cleavage assays to detect mutations triggered by engineered nucleases. *G3 (Bethesda)*, **5**, 407–415.
17. Kim,H., Um,E., Cho,S.R., Jung,C., Kim,H. and Kim,J.S. (2011) Surrogate reporters for enrichment of cells with nuclease-induced mutations. *Nat. Methods*, **8**, 941–943.
18. Kim,J.M., Kim,D., Kim,S. and Kim,J.S. (2014) Genotyping with CRISPR-Cas-derived RNA-guided endonucleases. *Nat. Commun.*, **5**, 3157.
19. Yu,C., Zhang,Y.G., Yao,S.H. and Wei,Y.Q. (2014) A PCR Based protocol for detecting indel mutations induced by TALENs and CRISPR/Cas9 in Zebrafish. *PLoS One*, **9**, e98282.
20. Bauer,D.E., Canver,M.C. and Orkin,S.H. (2015) Generation of genomic deletions in mammalian cell lines via CRISPR/Cas9. *J. Vis. Exp.*, **83**, e52118.
21. Brinkman,E.K., Chen,T., Amendola,M. and van Steensel,B. (2014) Easy quantitative assessment of genome editing by sequence trace decomposition. *Nucleic Acids Res.*, **42**, e168.
22. Brinkman,E.K., Kousholt,A.N., Harmsen,T., Leemans,C., Chen,T., Jonkers,J. and van Steensel,B. (2018) Easy quantification of template-directed CRISPR/Cas9 editing. *Nucleic Acids Res.*, **46**, e58.
23. Guell,M., Yang,L.H. and Church,G.M. (2014) Genome editing assessment using CRISPR Genome Analyzer (CRISPR-GA). *Bioinformatics*, **30**, 2968–2970.
24. Carrington,B., Varshney,G.K., Burgess,S.M. and Sood,R. (2015) CRISPR-STAT: an easy and reliable PCR-based method to evaluate target-specific sgRNA activity. *Nucleic Acids Res.*, **43**, e157.

25. Kc,R., Srivastava,A., Wilkowski,J.M., Richter,C.E., Shavit,J.A., Burke,D.T. and Bielas,S.L. (2016) Detection of nucleotide-specific CRISPR/Cas9 modified alleles using multiplex ligation detection. *Sci.Rep.*, **6**, 32048.
26. Tycko,J., Myer,V.E. and Hsu,P.D. (2016) Methods for optimizing CRISPR-Cas9 genome editing specificity. *Mol. Cell*, **63**, 355–370.
27. Kozlowski,P., Roberts,P., Dabora,S., Franz,D., Bissler,J., Northrup,H., Au,K.S., Lazarus,R., Domanska-Pakiela,D., Kotulska,K. *et al.* (2007) Identification of 54 large deletions/duplications in TSC1 and TSC2 using MLPA, and genotype-phenotype correlations. *Hum. Genet.*, **121**, 389–400.
28. Marcinkowska,M., Wong,K.K., Kwiatkowski,D.J. and Kozlowski,P. (2010) Design and generation of MLPA probe sets for combined copy number and small-mutation analysis of human genes: EGFR as an example. *Scientific World J.*, **10**, 2003–2018.
29. Schouten,J.P., McElgunn,C.J., Waaijer,R., Zwijnenburg,D., Diepvens,F. and Pals,G. (2002) Relative quantification of 40 nucleic acid sequences by multiplex ligation-dependent probe amplification. *Nucleic Acids Res.*, **30**, e57.
30. Kozlowski,P., Jasinska,A.J. and Kwiatkowski,D.J. (2008) New applications and developments in the use of multiplex ligation-dependent probe amplification. *Electrophoresis*, **29**, 4627–4636.
31. Ramlee,M.K., Yan,T.D., Cheung,A.M.S., Chuah,C.T.H. and Li,S. (2015) High-throughput genotyping of CRISPR/Cas9-mediated mutants using fluorescent PCR-capillary gel electrophoresis. *Sci. Rep.*, **5**, 15587.
32. Cradick,T.J., Fine,E.J., Antico,C.J. and Bao,G. (2013) CRISPR/Cas9 systems targeting beta-globin and CCR5 genes have substantial off-target activity. *Nucleic Acids Res.*, **41**, 9584–9592.
33. Cho,S.W., Kim,S., Kim,Y., Kweon,J., Kim,H.S., Bae,S. and Kim,J.S. (2014) Analysis of off-target effects of CRISPR/Cas-derived RNA-guided endonucleases and nickases. *Genome Res.*, **24**, 132–141.
34. Dabrowska,M., Juzwa,W., Krzyzosiak,W.J. and Olejniczak,M. (2018) Precise excision of the CAG tract from the huntingtin gene by Cas9 nickases. *Front. Neurosci.*, **12**, 75.
35. Serizawa,R.R., Ralfkiaer,U., Dahl,C., Lam,G.W., Hansen,A.B., Steven,K., Horn,T. and Guldberg,P. (2010) Custom-Designed MLPA using multiple short synthetic probes application to methylation analysis of five promoter CpG islands in tumor and urine specimens from patients with bladder cancer. *J. Mol. Diagn.*, **12**, 402–408.
36. Langerak,P., Nygren,A.O.H., Schouten,J.P. and Jacobs,H. (2005) Rapid and quantitative detection of homologous and non-homologous recombination events using three oligonucleotide MLPA. *Nucleic Acids Res.*, **33**, e188.
37. Lewandowska,M.A., Czubak,K., Klonowska,K., Jozwicki,W., Kowalewski,J. and Kozlowski,P. (2015) The use of a Two-Tiered testing strategy for the simultaneous detection of small EGFR mutations and EGFR amplification in lung cancer. *PLoS One*, **10**, e0117983.
38. Marcinkowska-Swojak,M., Handschuh,L., Wojciechowski,P., Goralski,M., Tomaszewski,K., Kazmierczak,M., Lewandowski,K., Komarnicki,M., Blazewicz,J., Figlerowicz,M. *et al.* (2016) Simultaneous detection of mutations and copy number variation of NPM1 in the acute myeloid leukemia using multiplex ligation-dependent probe amplification. *Mutat. Res.*, **786**, 14–26.
39. Ran,F.A., Hsu,P.D., Lin,C.Y., Gootenberg,J.S., Konermann,S., Trevino,A.E., Scott,D.A., Inoue,A., Matoba,S., Zhang,Y. *et al.* (2013) Double nicking by RNA-Guided CRISPR Cas9 for enhanced genome editing specificity. *Cell*, **154**, 1380–1389.
40. Fu,Y.F., Foden,J.A., Khayter,C., Maeder,M.L., Reyon,D., Joung,J.K. and Sander,J.D. (2013) High-frequency off-target mutagenesis induced by CRISPR-Cas nucleases in human cells. *Nat. Biotechnol.*, **31**, 822–826.
41. Yang,Z., Steentoft,C., Hauge,C., Hansen,L., Thomsen,A.L., Niola,F., Vester-Christensen,M.B., Frodin,M., Clausen,H., Wandall,H.H. *et al.* (2015) Fast and sensitive detection of indels induced by precise gene targeting. *Nucleic Acids Res.*, **43**, e59.
42. Findlay,S.D., Vincent,K.M., Berman,J.R. and Postovit,L.M. (2016) A Digital PCR-Based method for efficient and highly specific screening of genome edited cells. *PLoS One*, **11**, e0153901.
43. Gaudelli,N.M., Komor,A.C., Rees,H.A., Packer,M.S., Badran,A.H., Bryson,D.I. and Liu,D.R. (2017) Programmable base editing of A.T to G.C in genomic DNA without DNA cleavage. *Nature*, **551**, 464–471.
44. Sentmanat,M.F., Peters,S.T., Florian,C.P., Connelly,J.P. and Pruett-Miller,S.M. (2018) A survey of validation strategies for CRISPR-Cas9 editing. *Sci. Rep.*, **8**, 888.
45. Mock,U., Hauber,I. and Fehse,B. (2016) Digital PCR to assess gene-editing frequencies (GEF-dPCR) mediated by designer nucleases. *Nat. Protoc.*, **11**, 598–615.
46. Hellmann,I., Lim,S.Y., Gelman,R.S. and Letvin,N.L. (2011) Association of activating KIR copy number variation of NK cells with containment of SIV replication in rhesus monkeys. *PLoS Pathog.*, **7**, e1002436.
47. Armour,J.A.L., Palla,R., Zeeuwen,P.L.J.M., den Heijer,M., Schalkwijk,J. and Hollox,E.J. (2007) Accurate, high-throughput typing of copy number variation using paralogue ratios from dispersed repeats. *Nucleic Acids Res.*, **35**, e19.
48. Marcinkowska-Swojak,M., Klonowska,K., Figlerowicz,M. and Kozlowski,P. (2014) An MLPA-based approach for high-resolution genotyping of disease-related multi-allelic CNVs. *Gene*, **546**, 257–262.
49. Imbard,A., Pasmant,E., Sabbagh,A., Luscan,A., Soares,M., Goussard,P., Blanche,H., Laurendeau,I., Ferkal,S., Vidaud,M. *et al.* (2015) NF1 single and multi-exons copy number variations in neurofibromatosis type 1. *J. Hum. Genet.*, **60**, 221–224.
50. Gatta,V., Scarciolla,O., Gaspari,A.R., Palka,C., De Angelis,M.V., Di Muzio,A., Guanciali-Franchi,P., Calabrese,G., Uncini,A. and Stuppia,L. (2005) Identification of deletions and duplications of the DMD gene in affected males and carrier females by multiple ligation probe amplification (MLPA). *Hum. Genet.*, **117**, 92–98.